

Sorption behavior of Se(IV) species on kaolinite

Master's thesis

Jani Viitala

University of Helsinki

Department of Chemistry

## Abstract

Long term nuclear waste disposal has arisen as an important field of study due to the increasing amounts of generated nuclear waste. A suggested approach to long term disposal is geological waste deposits. Selenium-79 is a relevant radionuclide in nuclear waste because it has a long half-life and its species can be very mobile. Sorption modeling is a way of studying the sorption behavior in a very detailed manner. This study focused on sorption behavior of selenium on kaolinite, which is a prevalent clay mineral. Sorption was studied with batch sorption experiments, which yielded distribution coefficients and a sorption isotherm that details low sorption of selenium on the surface of kaolinite. Mineral characterization of kaolinite along with titration experiments resulted in promising sorption data, that could be further used for sorption modeling in the future.

## Table of contents

1. Introduction
  2. Background of the research
  3. Materials
    - a. Selenium
    - b. Kaolinite
  4. Sorption
  5. Modeling
  6. Experimental work
  7. Results and discussion
  8. Conclusion
  9. Future work
- References
- Appendices

## Abbreviations

2SPNE SC/CE          2 Site Protolysis Non-Electrostatic Surface  
Complexation and Cation Exchange -model

BET          Brunauer-Emmett-Teller; Method used to analyze specific  
surface areas of materials

CEC          Cation exchange capacity

CCM          Constant capacitance model

DDL          Diffuse double layer model

EDL          Electric double layer

ICP-MS      Inductively coupled plasma mass spectroscopy

MP-AES      Microwave plasma atomic emission spectroscopy

NEM          Non-electrostatic model

SSA          Specific surface area

SNF          Spent nuclear fuel

SCM          Surface complexation model

TLM          Triple layer model

XRD          X-ray diffraction spectroscopy

# 1. Introduction

Nuclear waste disposal has become a very important part in the nuclear fuel cycle assuring the safety of people and the environment<sup>1</sup>. Underground repositories deep in the bedrock are planned to store nuclear waste. Therefore, it is essential to know how the surrounding man made barriers and bedrock react to the radioactive waste, which can remain harmful for long time periods. In Finland, the KBS-3 method<sup>2,3</sup> is used for the final disposal of spent nuclear fuel in the Olkiluoto site.

Spent nuclear fuel (SNF) is usually comprised of many different radionuclides. This means that when deciding how to design the final disposal site, many factors need to be taken into account. Some radionuclides have long half-lives and others may have other chemical properties that make their final disposal complicated. Table 1 includes the radionuclides that are the most important to take into account when designing final disposal sites.

*Table 1, the most important radionuclides in high level waste in order of importance (top ones most important)<sup>4</sup>*

Radionuclide	Half-life	Mode of decay
C-14	5730 y	$\beta^-$
Cl-36	3.01e5 y	$\beta^-$ , e+ $\beta^+$
I-129	1.57e7 y	$\beta^-$
Mo-93	4.0e3 y	e
Nb-93m	16.13 y	IT
Nb-94	2.03e4 y	$\beta^-$
Cs-135	2.3e6 y	$\beta^-$
Ni-59	7.6e4 y	e+ $\beta^+$
Se-79	3.27e5 y	$\beta^-$
Sr-90	28.29 y	$\beta^-$
Y-90	64 h	$\beta^-$
Pd-107	6.5e6 y	$\beta^-$
Sn-126	1e5 y	$\beta^-$
Sb-126	12.46 d	$\beta^-$

One important radionuclide that needs to be considered is Se-79. Even though the amounts of Se-79 in the spent fuel are very low<sup>5</sup>, this nuclide is a long-living fission product so knowing how it behaves during its time in the final deposit is crucial. It is also a very significant source of radioactive doses over longer periods.

The main problem with selenium is its mobility. The two most common oxidation states for selenium are + VI and + IV. In these states, the selenium appears as either selenate ( $\text{SeO}_4^{2-}$ ) or selenite ( $\text{SeO}_3^{2-}$ ) respectively. In both of these forms, the sorption of selenium is very limited on different mineral surfaces<sup>6</sup>. Hence, studying the sorption of selenium in different chemical conditions is important. Sorption of selenium onto different mineral surfaces and diffusion has been studied before<sup>7-9</sup> but more information is required for a better understanding of the behavior of selenium in different mineral matrices.

The most important minerals are alteration products of granitic rock main minerals that exist next to the fractures in the rock<sup>10</sup>. Sorption of selenium onto clay minerals, such as kaolinite, is paramount when considering the final disposal of SNF that might release selenium into the repository surroundings.

Sorption of selenium on kaolinite and illite was studied before<sup>11</sup> but current information is still quite limited. The objective of this study was to further study the sorption of selenium on kaolinite due to its importance in geological repositories. Simulating the actual geological environment was an important detail when conducting the experiments. Sorption was studied with batch experiments<sup>12,13</sup>. Kaolinite was characterized by measuring the mineral composition, specific surface area and the cation exchange capacity. To better describe the sorption of selenium in different conditions, titration experiments were performed to obtain a proper surface complexation model. Titration results were further calibrated by measuring the proton- and cation exchange on kaolinite. The parameters that were obtained can be used to support modeling work in the future. Different modeling approaches are discussed more in detail in the literature survey.

## 2. Background of the research

Currently, nuclear energy provides 11% of the entire world's electricity needs with over 450 reactors with more being built. The energy from the nuclear reactors is produced with nuclear fission. Fuel for the fission is provided mainly by uranium, specifically its isotope U-235. Other nuclei are also used as fuel, such as Pu-239. A number of fissile nuclei are bombarded with neutrons, until one nucleus undergoes fission and causes a chain reaction. The nuclear reaction then produces two smaller nuclei. For example, U-235 nucleus can produce Kr-92 and Ba-141 nuclei along with gamma rays and neutrons. These nuclei are called fission products.

Eventually the chain reactions stop and what is left is the fission products and the rest of the unused fuel. This spent nuclear fuel has to be properly handled and disposed.<sup>14</sup>

SNF consists of lots of different components. Most of the spent fuel consists of uranium and the rest is formed by varying fission products. Since these fission products can vary from gas products to metals and lanthanides to transuranium elements, SNF can remain active for thousands, or even millions of years and it may change over time. Therefore, long term solutions are required. One solution that stands out over others is geological repositories.<sup>14</sup>

Long term disposal has to be designed and managed so that the environment and humans stay safe. Currently geological repositories are the only option for this. Repositories require a stable geological environment.

The conditions in the spent fuel change over time. As the radioactive materials decay, the composition of the fuel change and so does its chemical properties. This has to be taken into account when considering final disposal. When the fuel is deposited underground we need to consider how the changes in the waste affect its surroundings. In this case the rock covering the repository is surrounding the deposited waste. So how the changes in the spent fuel affect the surrounding rock is crucial information. Since the most important thing about storing the spent fuel is avoiding harm to the environment and people, it is extremely important to know how the surrounding rock is affected.

Groundwater is an important factor in the system. If it would come to it that radioactive material is released into groundwater, many more hazards become relevant. This could compromise drinking water and directly affect people. This creates a whole another set of problems that need to be solved, which is why this scenario has to be avoided at all costs.

What this essentially means is that we need to know if the radionuclides can penetrate the surrounding rock or not. Many different factors come into play here including the mobility of the nuclides and retention of the nuclides on the rocks. Because the spent fuel can contain various different nuclides with different properties, knowing how these nuclides react in different environments is important. Some nuclides may be shorter lived and other nuclides could have half-lives of millions of years so they stay harmful for longer. The activity of the major radionuclides relative to each other can be seen in figure 1<sup>15</sup>. The figure does not include all the possible nuclides that are relevant but it gives a general idea of the timescales and the

amount of activities that have to be dealt with. How important these nuclides are depends then on how they act during their time in the repository. Some nuclides, such as Se-79, are very mobile so if they also have a long half-life, they have a long time of potentially trying to penetrate the surrounding rock.<sup>16</sup>

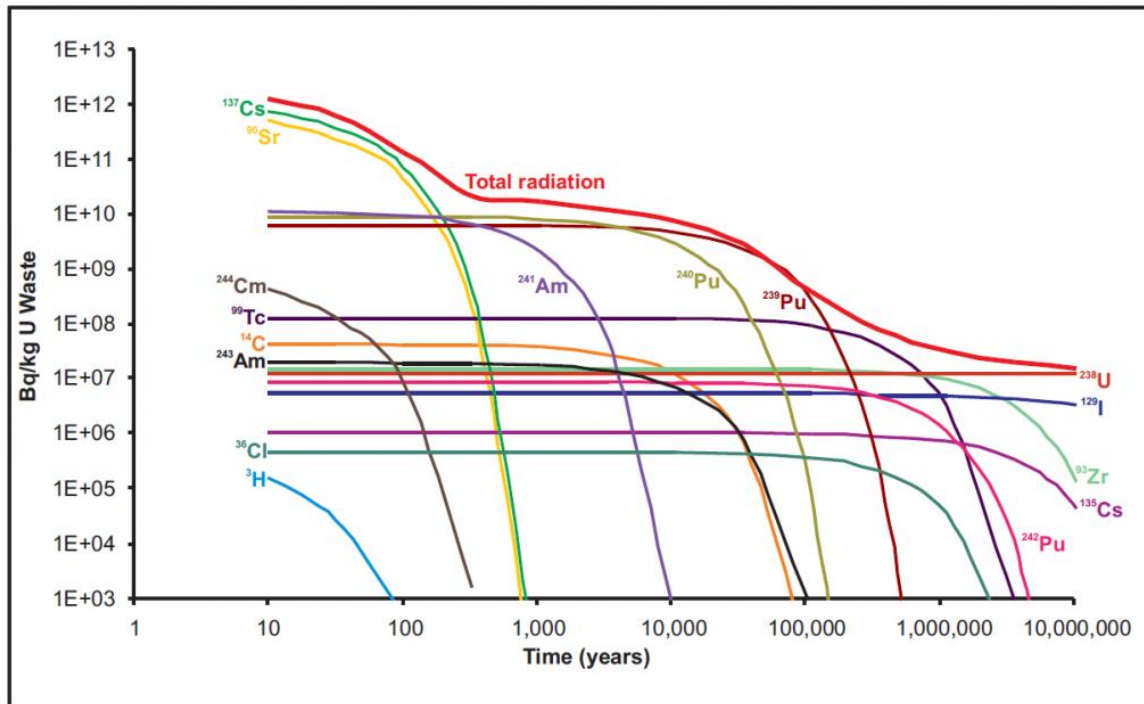


Fig 1, Figure of relative activity of major isotopes in radioactive waste<sup>15</sup>

In Finland, the geological disposal of spent nuclear fuel is done at the Olkiluoto site. The site was chosen because the region is stable and the bedrock is very old in geological timescales and in good condition. The disposal is done with the KBS-3 method. In this method, the spent nuclear fuel is stored deep within the Olkiluoto bedrock and encapsulated in sealed canisters in the underground repository<sup>17</sup>. This method ensures that the release of radionuclides is prevented with both the engineered containers and barriers, along with the surrounding bedrock. This produces a safety concept that is sufficient for the long-term disposal of SNF<sup>17</sup>.

To be specific, the disposal method is called the KBS-3V method. This is because the canisters are placed vertically, compared to the KBS-3H method<sup>18</sup> where they are placed horizontally. The general concept of the method is shown in figure 2. As mentioned above, the method is designed around multiple layers of barriers. The first barrier is the copper canister where the



SNF is first stored. The SNF is placed into iron inserts, which are then enclosed in the canister. Iron is chosen for its strength and the copper overlay for the corrosion resistance so the canister can isolate the fuel for as long as it stays harmful<sup>19</sup>. The second layer is a bentonite buffer. Bentonite clay is used to protect the canisters from any external process that could affect the containers and to limit the spread of radionuclides in case of leakage. The deposition tunnel is then backfilled with clay and bentonite blocks. This provides additional protection for radionuclide leakages. Closure will then completely isolate the fuel. The intention is to completely close off the disposal site with backfill materials. This way the disposal site will be completely sealed from people and the environment will stay favorable and predictable.<sup>19</sup>

The final barrier is the host rock. The host rock isolates the disposal site from the inhabitants above and provides the solid and stable conditions for the other barriers. As the final barrier, it will also limit the release of radionuclides into the environment and so studying the flow, diffusion and sorption of radionuclides in the host rock environment becomes important<sup>19</sup>. The host rock consists of different minerals and so knowing how exactly different radionuclides migrate within the rock can get complicated.

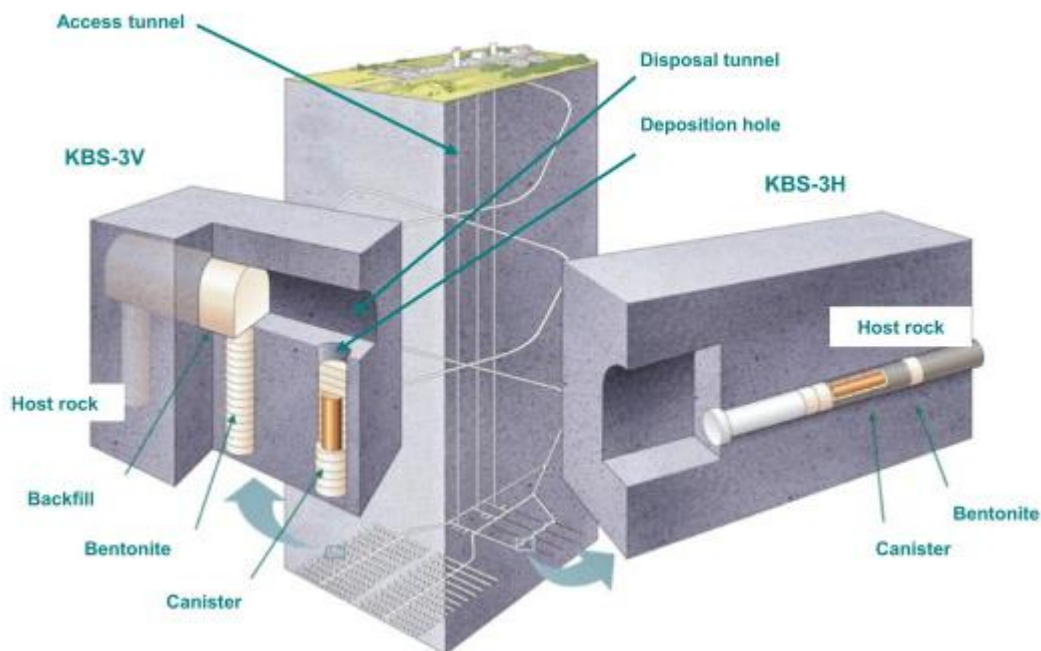


Fig 2, Schematic figure of the KBS-3 concept repository<sup>18</sup>

### 3. Studied materials

#### 3.1 Selenium

Selenium is a nonmetal element with the atomic number of 34. In nature, it appears mostly as a salt instead of its elemental form. Selenium has four common oxidation states that it forms salts with: -II, +IV and +VI. Speciation of selenium can be seen closer in figure 3<sup>6</sup>. The most common forms of selenium that occur in nature are various selenides, selenites and selenates.

Selenium in trace amounts is required for cellular functions but in larger doses, it becomes toxic. Selenosis is possible when exceeding an intake of 400 micrograms of selenium per day<sup>20</sup>. While elemental selenium is not very toxic, selenates and selenites are instead very toxic<sup>21</sup>. Hydrogen selenide is also a toxic gas.

Selenium has several relevant isotopes. It has five stable isotopes: <sup>74</sup>Se, <sup>76</sup>Se, <sup>77</sup>Se, <sup>78</sup>Se and the most abundant <sup>80</sup>Se. Two radionuclides also occur naturally: <sup>82</sup>Se and <sup>79</sup>Se. Another important radionuclide is <sup>75</sup>Se. Of the radioisotopes, the most interesting one is <sup>79</sup>Se. It is mostly produced in the process of nuclear fission of uranium in small quantities and as an activation product of the stable <sup>78</sup>Se. The isotope is a beta emitter, specifically  $\beta^-$ -emitter with almost no other emission.

As a fission product, <sup>79</sup>Se is a relevant radionuclide in spent nuclear fuel<sup>14</sup>. With a half-life of 327 000 years and high mobility, <sup>79</sup>Se is an important radionuclide when considering final disposal of spent nuclear fuel<sup>6</sup>. It has also been noticed to be a significant source of activity<sup>22</sup>. However, the speciation of selenium in SNF is not known. A variety of redox states could exist in the SNF. This causes a problem, because the mobility of selenium is highly dependent on its oxidation state<sup>12</sup>. If multiple different forms of selenium exist in the matrix, it becomes difficult to know exactly how the selenium behaves.

In oxidizing conditions, selenium appears as its +VI form selenate ( $\text{SeO}_4^{2-}$ ) and in slightly less oxidizing conditions as a +IV form selenite ( $\text{SeO}_3^{2-}$ ). In these conditions, the selenium is very mobile. In contrast, if selenium exists at lower redox potentials, it is found in its elemental form or as selenide ( $\text{Se}^{2-}$ ) which forms insoluble salts<sup>6</sup>. In these forms selenium is not mobile

at all because of their low solubility. The reduction reaction in itself is slow because the reaction requires the transfer of multiple electrons<sup>16,23</sup>.

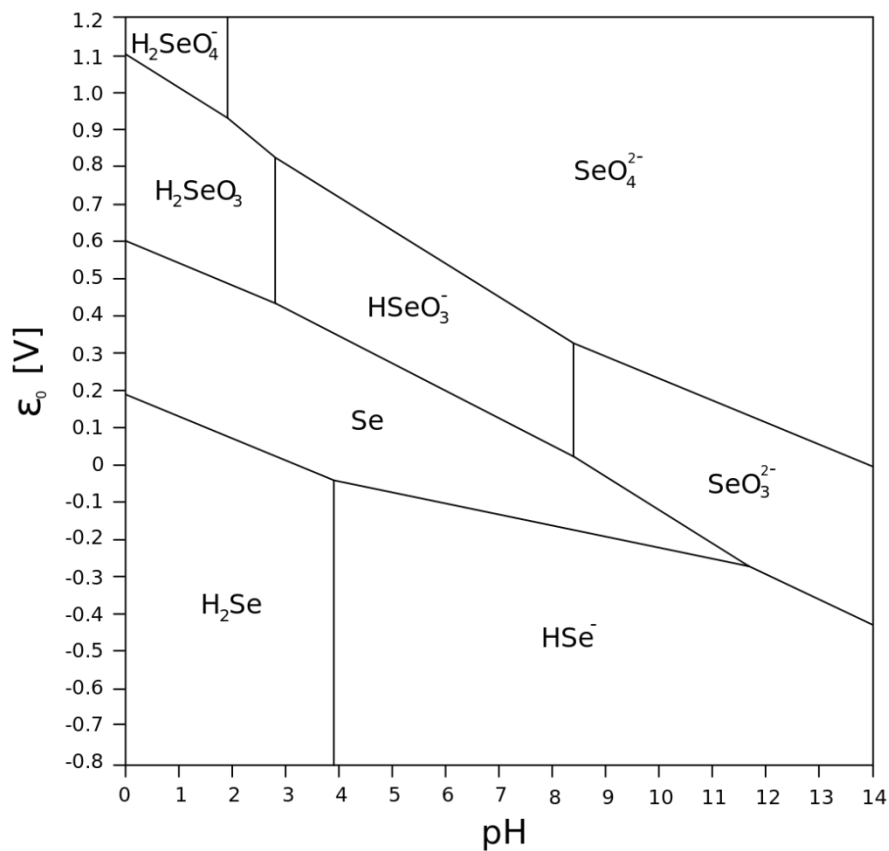


Fig 3, Eh/pH diagram of selenium species (Wikimedia Commons)

In geological repositories, the SNF is surrounded by vast amounts of rocks and minerals. As established above, within the SNF, selenium is going to be in multiple different forms. The chemical conditions of the surrounding groundwater affect the Eh/pH conditions of the disposal site a lot. This means that most of the selenium is likely in a very mobile form due to the slow reduction process. If selenium manages to reach the surrounding rock, it must be ensured that it cannot breach the rock barrier. For this, studying the sorption of selenium on different mineral surfaces is important. Again, this is complicated by the fact that selenium likely exists in multiple forms within the SNF.

The main mechanism of retention for selenate is outer sphere complexation. This form of sorption is weak and therefore selenate sorption onto mineral surfaces is low<sup>23</sup>. Selenite on the other hand forms inner sphere complexes in which selenite forms a chemical bond

between the oxyanion and the metals on the mineral surface. This type of sorption is a lot stronger<sup>23</sup>. The surface complexation is detailed further in chapter 4.

### 3.2 Kaolinite

Kaolinite is a clay mineral with a chemical formula of  $\text{Al}_2\text{Si}_2\text{O}_5(\text{OH})_4$ . It is heavily localized in the Gaoling area in China, for which it was also named after. Its occurrence is however not limited to just China and it is instead spread thoroughly in Asia, Europe and North America. Kaolinite is formed usually in chemical weathering of aluminum silicates. It is a relatively soft mineral, usually white in color. Its crystal system is triclinic, in which the crystal structure is described with three basis vectors that are all different lengths and have different angles between them. However, kaolinite rarely crystallizes and is instead found usually in clay bed masses<sup>24</sup>. The crystal structure of kaolinite can be seen in figure 4.

The cation-exchange capacity (CEC) of kaolinite has been studied before<sup>25</sup> and it has been noted to be relatively small. The CEC is mostly caused by the surface charge of kaolinite. Increased particle size and higher pH values increase the CEC. In some cases, a high CEC value can be found in kaolinites that have smectite layers on the surface of kaolinite.

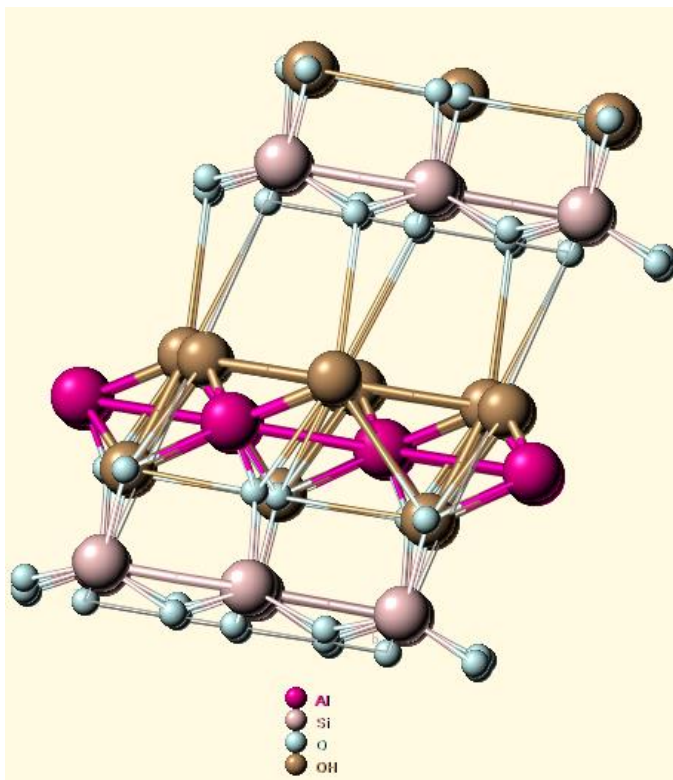


Fig 4, Crystal structure of kaolinite<sup>26</sup>

Sorption on kaolinite has also been studied a lot due to its prevalence in rocks and soils in geological waste disposal sites. The layer structure of kaolinite causes it to have a strong sorption capacity compared to the low CEC. The sorption of various radionuclides on kaolinite has been studied, including but not limited to: uranium<sup>27</sup>, selenium<sup>28</sup> and europium<sup>29</sup>. For selenium specifically, it was noted that coating kaolinite with either iron or aluminum increased the sorption of selenium<sup>30</sup>.

## 4. Sorption

When substances attach onto one another by different mechanisms, it is called sorption. Sorption entails the three different methods, which are absorption, adsorption and ion exchange. In absorption, one substance takes in another substance whereas in adsorption, a substance is attached onto another substance's surface. In ion exchange, surface substances exchange cations or anions between themselves<sup>31</sup>.

Sorption is relevant in many naturally occurring systems, which makes it an important field of study. Adsorption specifically is a main form of retention in soils. Studying sorption on soils can therefore give information on mobility of substances and the chemical conditions of the soil. The distribution of the substances in the soil (or any other solid media) is described by the distribution coefficient  $K_d$ . Distribution coefficient is defined as following:

$$K_d = \frac{c_s}{c_{aq}} \quad (1)$$

where  $c_{aq}$  is the concentration of the substance in aqueous phase and  $c_s$  is the concentration of the substance in a solid phase, such as soil. The value of the distribution coefficient depends strongly on the environment.

Sorption occurs on the surface of any reactive substance. The surface functional group is prone to reacting with any ion that it comes in contact with. When this happens, surface complexes are formed. Two types of surface complexes exist. A stronger inner-sphere complex and a weaker outer-sphere complex. An example of both types of complexation can be seen in figure 5.

Outer-sphere complexes are formed and maintained by electrostatic charges, with no direct bonding between the reacting substances. Instead, molecules of the aqueous media, such as

water, exist between the bonding substances. The water molecules prevent the bonding substances from forming direct bonds with each other and therefore forming a weaker bond. This form of retention is weak and the retained molecules are easily displaced. The displacement of retained molecules is commonly known as ion exchange. Ion exchange is a significant retention mechanism for most ions<sup>32</sup>.

Inner-sphere complexes are formed with a direct chemical bond between the reacting ion and the surface ligand. The complexation is further described by two terms. The first term, either monodentate or bidentate, describes the amount of positions in the coordination sphere that are involved in the sorption of the adsorbing substance. Monodentate means that there is one position occupied and likewise bidentate means two positions are occupied. The second term describes the amount of metal atoms that take part in the bonding. Mononuclear means there is one metal atom involved and binuclear if there is two.

If the surface coverage is low, metals usually form monodentate complexes and as the surface coverage increases, bidentate complexes get more common. Inner-sphere complexes are common for the first row of transition metals and some heavier metals. Unlike outer-sphere complexes, inner-sphere complexes are relatively stable.

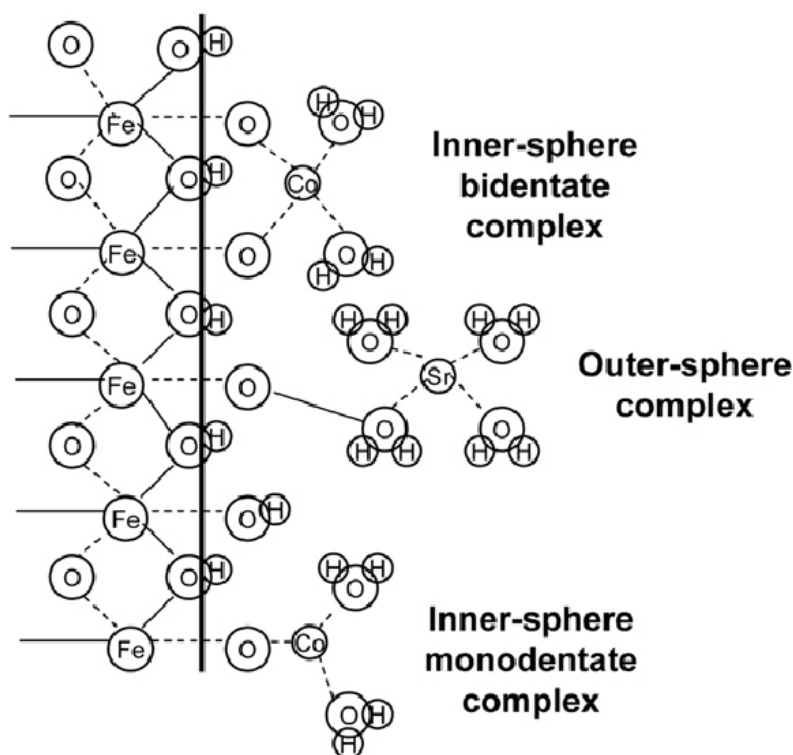


Fig 5, An example of the different types of surface complexation. The difference between outer-sphere and inner-sphere complexes is very noticeable.<sup>33</sup>

On mineral surfaces, two types of surface charge can develop. These are permanent charge or pH dependent charge. Permanent charge is formed when the mineral crystallizes and is no longer able to be changed by the environment's chemical properties. It is a result of isomorphic substitution and is specific to phyllosilicates such as kaolinite. The isomorphic substitution usually results in the silicates having a negative charge due to the substitution of cations. The substitution is therefore a defining characteristic in classifying layered clay minerals<sup>31</sup>.

The sorption site of the silicate surface caused by the isomorphic substitution is located in a cavity within the hexagonal structure of the siloxane. In the cavity, three oxygen atoms are able to react with sorbed metals. Depending on how the electric charges are distributed in the layers, the reactivity of the cavity will differ. If a permanent negative charge is close to the cavity, the reactivity will depend on the isomorphic substitution and in which layer it occurs. The charge will then be distributed differently based on the location of the isomorphic substitution<sup>31</sup>.

The other type of surface charge is pH-dependent. It is a result of the combination of the mineral surface and the mineral's environment. This type of surface charge works mainly around the hydroxyl groups ( $\equiv\text{SOH}$ , where S is a metal) on the mineral surface. These hydroxyl groups either protonate or deprotonate depending on the amount of metal atoms the hydroxyl groups are coordinating with. Valency and coordination of the metal atoms also affect the reactivity. Because of the pH dependency of the charge, the surface charge can be either positive or negative. However, at certain pH values, the surface charge is zero. This is known as the point of zero charge (PZC)<sup>31</sup>.

Charge density describes how much electric charge is distributed on a given surface. Intrinsic surface charge density  $\sigma$  of a given mineral is defined as:

$$\sigma = \frac{F(q_+ - q_-)}{A} \quad (2)$$

where F is the Faraday constant,  $q_+$  and  $q_-$  are the amounts of adsorbed cations and anions respectively and A is the area of the mineral surface. At PZC, the charge density will be zero.

The interface between the solid and solution phase is a region that consists of layers, which differ with each other in both chemical and electrochemical characteristics. This interface

region is affected by characteristics of both the solid media and the solution phase. Surface models can further describe the solid-solution interface. Because of the adsorption, a layer is formed on the mineral surface by the charge. A second layer forms in the solution by the ions of the opposite charge. This is known as the electric double layer (EDL)<sup>31,34</sup>. An example of an EDL model would be the Helmholtz model that can be seen in figure 6. In this model, the negative charge is evenly distributed on the mineral surface and the opposing positive charge in the solution exists in parallel to the surface. The surface potential decreases as the distance of the opposing ions increase<sup>31,34</sup>.

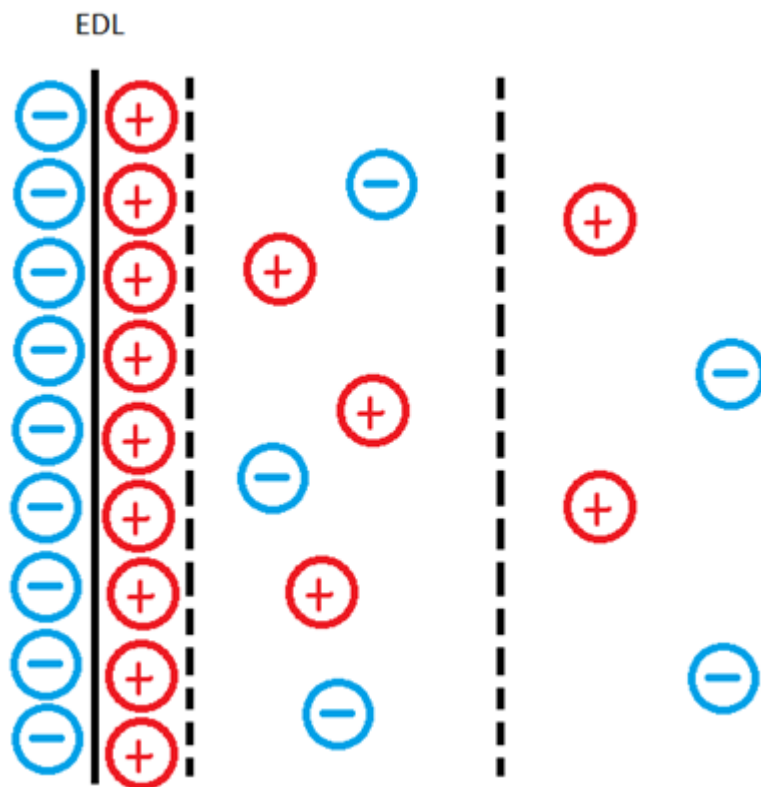


*Fig 6, a rough visual presentation of EDL. The figure shows the charge density lowering as the distance from the first layer increases*

Sorption and its pH dependency can be visually presented by plotting the amount of a sorbed substance onto another at different pH values. Specifically, the pH where half of the metal is sorbed is known as the sorption edge<sup>31</sup>. These figures show how quickly the adsorption



increases at the sorption edge. An example of a sorption edge can be seen in figure 7. In the figure,  $f_{\text{sorb}}$  describes the fraction of the total metal ion amount that is adsorbed.

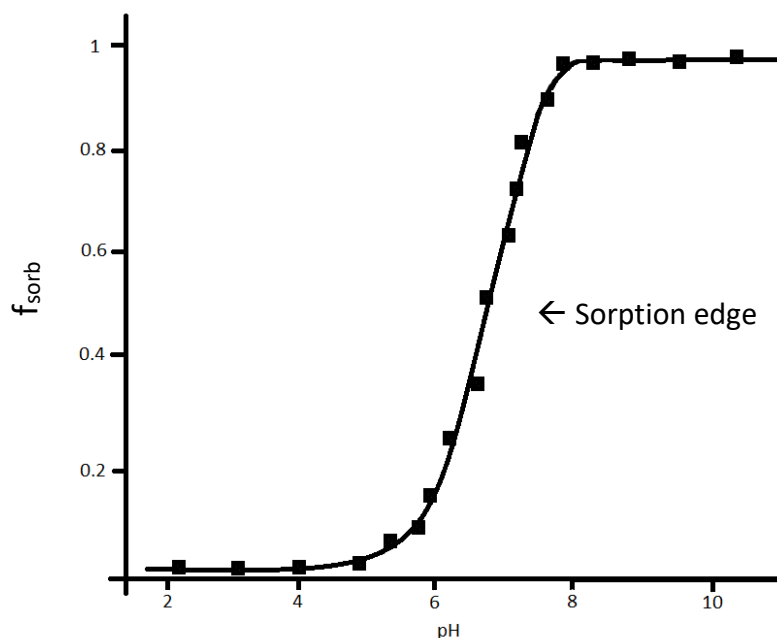


Fig 7, An example of a sorption figure. Sorption edge at the point when 50% of the metal has been sorbed on the mineral surface. Rapid increase in metal adsorption is very noticeable at the sorption edge.

Since selenium is an important radionuclide in SNF, the sorption of selenium on different minerals has been studied extensively. As mentioned above, selenium mobility is reliant on the oxidation states. The most mobile forms are selenate and selenite. Selenate forms outer-sphere complexes and selenite forms inner-sphere complexes. Because of the outer-sphere complexation of selenate, its retention is considered low<sup>35</sup>. However, selenate has been noted to form inner-sphere complexes in few cases on minerals such as goethite<sup>36</sup>.

Selenite on the other hand can form different types of inner-sphere complexes. It has been studied that selenite can form both mononuclear-monodentate and binuclear-bidentate complexes. Mononuclear-monodentate complexes has been observed to form on magnetite surface<sup>37</sup> and binuclear-bidentate complexes on goethite<sup>37,38</sup>. Some metals can increase the retention of selenium by contributing to the reduction of selenium. Iron and aluminum have both been noted to have this effect<sup>28,37</sup>. Outer-sphere complexation also happens, but inner-sphere complexation remains as the more dominant adsorption method<sup>31,39</sup>.

Selenite sorption and diffusion in granite was studied by Ikonen et al. to determine distribution and diffusion coefficients in granite and to get more information about the retention of selenium in granitic rocks<sup>8</sup>. Low  $K_d$  values indicated poor retention for selenate and a bit higher retention for selenite under nitrogen atmosphere. Sorption experiments were carried out under atmospheric conditions and in a glove box under nitrogen atmosphere to study the effect of low oxidizing environment on selenium sorption, same as Li et al. did in their work<sup>12</sup>. Yang et al. observed similar results but they also noted that biotite in granitic rocks had higher retention for selenium<sup>40</sup>. This is explained by the existence of iron(II) in the biotite structure.

Li et al. further studied selenium sorption on biotite and the  $K_d$  values were noticeably higher on biotite than other main minerals of the studied Grimsel granodiorite<sup>12</sup>. Specific surface area of the biotite was noted to be an important factor when sorption behavior between the minerals was compared. In addition, their modeling work suggests that biotite has three working sorption sites, which all work a bit differently depending on the selenium concentrations.

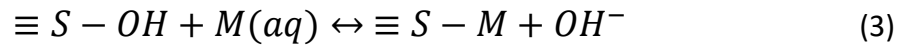
## 5. Modeling

Sorption can be further described with adsorption isotherms. They are a common way to express the amount of a compound that has been sorbed onto another's surface compared to the total amount of the adsorbing compound at a fixed temperature, pressure and pH in solution. Two different isotherms are commonly used: Langmuir and Freundlich isotherms<sup>41</sup>.

The Langmuir isotherm is the simpler one. Langmuir isotherm explains sorption by assuming the adsorbent is a gas that adsorbs onto a solid surface. Some assumptions are made for the model:

- Solid surface is homogenous -> sorption sites are identical
- Sorption site can hold at most one adsorbent molecule -> a monolayer of adsorbent molecules is formed
- The adsorbent molecules do not interact
- Surface equilibrium

When these qualities are met, the system follows the Langmuir equation. The equation is derived from the general adsorption reaction equation, which goes as following:



$\equiv S$  represents a sorption site in the solid surface,  $M$  is the adsorbing substance and  $OH$  is a hydroxyl group. The reaction can be further described by equilibrium constant  $K$ , which is defined as:

$$K = \frac{(\equiv S - M)(OH^-)}{(\equiv S - OH)(M)} \quad (4)$$

The Langmuir equation itself is the following:

$$q = \frac{bKc}{(1+Kc)} \quad (5)$$

where  $q$  is the amount of substance that has been adsorbed,  $b$  is the maximum amount of sorption sites,  $K$  is the equilibrium constant and  $c$  is the total concentration of adsorbents in the solution. According to the equation, the sorption sites become fully saturated after all the sorption sites are occupied by the monolayer coverage. This means that no more sorption can happen even if more adsorbing substance is added to the system.

Freundlich isotherm is a bit different in the sense that the Freundlich isotherm is not formed on a theoretical basis. Instead, it is an empirical relation between the adsorbent concentration on mineral surface and the total concentration of the adsorbent in the solution. The equation goes as following:

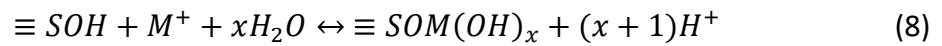
$$q = K_F c^N \quad (6)$$

where  $q$  again is the adsorbed substance amount,  $c$  is the substance concentration in the solution and  $K_F$  and  $N$  are constants depending on the adsorbent.  $N$  is usually smaller than one so it takes into account that the substance is removed from the solution and adsorbed on the mineral surface<sup>42</sup>. The equation can be further linearized with logarithm to better fit experimental data:

$$\log q = \log K_F + N \log c \quad (7)$$

The isotherms themselves do not indicate anything about the retention mechanisms. Since the adsorption system can get very complicated if more substances are added into the system, it is necessary to create models to better understand the chemistry of the system and the adsorption behavior. Surface complexation models (SCM) were created for this very purpose and they are helpful in identifying the reactions and equilibrium constants of the adsorption system. They are especially useful for predicting the distribution of the substance between the solution and adsorbent phase. Different models have been developed with varying concepts of charge distribution, electrical potential and the location of the adsorbed species<sup>31</sup>.

The general form of a surface complexation equation usually looks like the following:



and the corresponding  $K_M$ , the surface stability constant, is defined as:

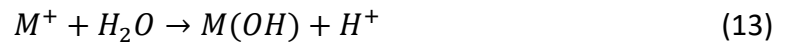
$$K_M = \frac{\{\equiv SOM(OH)_x\}*(H^+)^{(x+1)}}{\{\equiv SOH\}*(M^+)} \quad (9)$$

In addition to these, protolysis and hydrolysis reactions happen. Protolysis reaction, deprotonation and the protonation constant can be defined as:



$$K_+ = \frac{[\equiv SOH](H^+)}{[\equiv SOH_2]} \quad (12)$$

And the hydrolysis reaction of the metal is defined similarly:



$$K_{M(OH)} = \frac{(M(OH))*(H^+)}{(M^+)} \quad (14)$$

These equations form the basis for all sorption reactions.

All the different models also follow some basic assumptions<sup>31</sup>:

- Mineral surfaces in aquatic environment contain well defined functional groups
- Total concentration can be defined for all the different surface sites
- For every adsorption event, an adsorption energy can be defined

In addition, all the models require similar parameters that need to be figured out, either experimentally or from existing literature. Specific surface area of the mineral, sorption site types and site concentrations are the most important values. EDL parameters are also often required. Finally, complexation constants are experimentally determined<sup>43</sup>.

Non-electrostatic model (NEM) is the most basic model. As such, it requires the least amount of adjustable parameters. The name comes from the fact that no EDL parameters are required because no electrostatic corrections are made<sup>44</sup>. This means that only the chemical reactions have any effect on the model. Equations 8-14 essentially form the entire basis for NEM and it just becomes a case for solving the equations for different adsorption systems.

This might give the impression that the NEM is not able to properly express the sorption event. However, there are cases where this type of simple model is sufficient enough to describe the sorption edges and isotherms in varying conditions. Arora et al. did a comparison between an electrostatic and a non-electrostatic model for uranium sorption and found that while the NEM is highly pH dependent and the applicability changes over time, it is still a valid option<sup>45</sup>. The NEM did not yield clearly worse results and because of its easier development, it might be preferable to an electrostatic model.

Bradbury and Baeyens took a different approach and developed a NEM a bit further<sup>44</sup>. Their 2 Site Protolysis Non-Electrostatic Surface Complexation and Cation Exchange (2SPNE SC/CE) model was able to describe sorption for multiple different metals on montmorillonite surface in different chemical environments. They noted that sorption competition might be an issue for the model and modeling systems with multiple metals competing for sorption has to be specified well. They also brought up the problem of modeling systems that are more complex, which was not possible with the model.

Constant Capacitance Model (CCM) is a more standard electrostatic model that employs the general parameters, including the electrostatic corrections. The sorption is assumed to

happen in a single surface layer. Because of this, only inner-sphere complexes are assumed to happen<sup>31</sup>. CCM has mostly been used to describe systems of high ionic strength because of its requirement for specific ionic strengths. What makes CCM different to other electrostatic models is the capacitance value. The capacitance value changes how the surface charge  $\sigma$  is defined:

$$\sigma = \frac{C \cdot A \cdot q}{F} * \Psi \quad (15)$$

where C is the capacitance value, A is the surface area, q is the concentration of the adsorbent, F is the Faraday constant and  $\Psi$  is the surface potential. The capacitance value itself is usually experimentally determined and then optimized to fit the data. To actually use the modified surface charge, intrinsic adsorption constants need to be defined.

The intrinsic adsorption constant is defined with the combination of the regular adsorption constant and the coulombic part, so the equation looks like the following:

$$K^{int} = K * K_{coul} \quad (16)$$

The coulombic part can be defined with surface potential and surface charge:

$$K_{coul} = e^{\frac{-F\Delta Z\Psi}{RT}} \quad (17)$$

where F is the Faraday constant,  $\Delta Z$  is the net surface charge,  $\Psi$  is the surface potential, R is the ideal gas constant and T is the temperature. For protolysis reaction and the corresponding adsorption constant, the intrinsic adsorption constant is defined as:

$$K_+^{int} = \frac{[\equiv SOH](H^+)}{[\equiv SOH_2]} * e^{\frac{F\Psi}{RT}} \quad (18)$$

For this particular reaction, the surface charge is equal to one and as such is not seen in the equation for the intrinsic constant. Equation 18 forms the basis for all the electrostatic effects for adsorption events. For NEMs the surface charge  $\Delta Z$  is zero, so that explains why the NEM equations are more simple.

The next equations to be considered are the mass and charge balance expressions<sup>31</sup>. These equations take into account all the possible reactions that happen in the adsorption system and express the mass and charge distribution. The mass balance  $S_T$  expression is defined as:

$$S_T = [\equiv SOH^0] + [\equiv SOH_2^+] + [\equiv SO^-] + [\equiv SOM^{m-1}] + [\equiv SL^{1-n}] + 2[(\equiv SO)_2M^{m-2}] + 2[\equiv S_2L^{2-n}] \quad (19)$$

And the charge balance  $\sigma_0$  expression is similarly defined:

$$\sigma_0 = \frac{F}{q * S_A} \{ [\equiv SOH^0] + [\equiv SOH_2^+] + [\equiv SO^-] + (m-1)[\equiv SOM^{m-1}] + (1-n)[\equiv SL^{1-n}] + (m-2)[(\equiv SO)_2M^{m-2}] + (2-n)[\equiv S_2L^{2-n}] \} \quad (20)$$

where  $c$  is the concentration of the adsorbent and  $S_A$  is the specific surface area. The equations take into account all the possible reactions in the sorption system, including protolysis, metal sorption, ligand sorption and bidentate surface complexation reactions. If we now take into account equation 15, surface potential can be determined for a generic system as:

$$\Psi = \frac{F * \sigma_0}{c} = \frac{F^2}{q * c * S_A} \{ [\equiv SOH^0] + [\equiv SOH_2^+] + [\equiv SO^-] + (m-1) * [\equiv SOM^{m-1}] + (1-n) * [\equiv SL^{1-n}] + (m-2) * [(\equiv SO)_2M^{m-2}] + (2-n) * [\equiv S_2L^{2-n}] \} \quad (21)$$

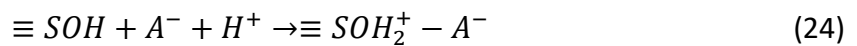
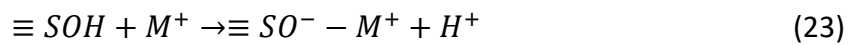
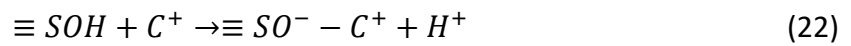
Lützenkirchen studied applications for CCM<sup>46</sup>. In his study, he acknowledged the fact that CCM has been mainly used for systems with high ionic strength, because of the high specificity of the model. Since there have been cases of CCM being used to describe systems of lower ionic strength, he wanted to note that while the results from the modeling look appealing, they are at odds with the relations of the solid-electrolyte surface. This makes the results obtained under low ionic strength look feasible, but physically they make no sense. In conclusion, CCM works best at specific high ionic strength environments.

Goldberg and Suarez used a CCM in practice in their study of anion sorption in soil systems<sup>47</sup>. In their study, they were successful in obtaining proper data with the model. They were able to model the sorption and transport of boron, molybdenum and arsenic in soils. Gabos et al. did a similar study for selenium sorption in tropical soils<sup>48</sup>. Their model showed results where

selenate sorption was very low at all the pH values but selenite sorption was instead very high and correlated with the iron and aluminum concentration in the soils. Because selenate forms mostly outer-sphere complexes, their model required some optimizations of the surface complexation constants for the selenate sorption.

Triple layer model (TLM) is different from the previous models because it can predict and model sorption happening on multiple surface layers. This allows TLM to be able to model both inner-sphere and outer-sphere complexation. The layers, or planes, are consecutively placed from the solid surface<sup>49</sup>. Inner-sphere complexes are located in the first plane and the outer-sphere complexes in the second plane. The final diffuse layer is formed by electrostatic interactions with surface ions. These different layers allow a better presentation of the charge separation in the triple layer configuration. This combined with the fact that TLM offers a relatively simple way of representing surface sites makes it a very popular option for surface complexation modeling.

The basis of the TLM is similar to the CCM, following the same equations for the different reactions 8-14, but in addition to those, it can take into account the outer-sphere complexation and the corresponding reactions:



where  $C^+$  and  $A^-$  are the background cation and anion respectively. The intrinsic adsorption constants for these reactions are formed according to equation 18.

What is also different for TLM is that for each plane, a surface potential is defined by the capacitance values in the following way:

$$\sigma_{is} = C_1(\Psi_{is} - \Psi_{os}) \quad (25)$$

$$\sigma_d = C_2(\Psi_d - \Psi_{os}) \quad (26)$$

Equation 25 describes the inner-sphere surface potential and equation 26 the diffuse layer potential with the adjustable inner layer capacitance  $C_1$  and outer layer capacitance  $C_2$ .<sup>31</sup> The mass and charge balance equations are also formed in the same way as equations 19 and 20.



Because of its flexibility of being able to model both inner-sphere and outer-sphere complexes, TLMs are widely used for different sorption environments. Selenite forms both types of surface complexes, so TLM would be a valid choice for modeling selenite sorption on different solid surfaces. Goldberg did just that for a wide variety of clay minerals, oxides and different soils<sup>50</sup>. Successful fittings of selenite sorption were obtained, with the modeling results agreeing with both previous observations and comparisons to other similarly adsorptive substances such as molybdenum. Also according to the model, selenite mostly forms inner-sphere complexes at lower pH values and outer-sphere complexes at higher pH values.

## 2SPNE SC/CE

The 2 Site Protolysis Non-Electrostatic Surface Complexation and Cation Exchange -model developed by Bradbury and Baeyens has recently risen in popularity due to its extreme flexibility and accuracy. It was originally based on a Diffuse Double Layer (DDL) model and then modified further to better fit their experimental data.<sup>51,52</sup>

In their study of Ni, Ca and Zn sorption on Na-montmorillonites, their initial plan was to use a DDL to model the experimental data<sup>51</sup>. When the DDL model proved insufficient, they looked to find out why the model would not work. Their conclusion was that the electrostatic term caused problems in their calculations instead of the surface complexation reactions or the other parameters. Therefore, they decided to completely forget the electrostatic term in their model and instead focus on improving the model by other methods. Next, they would decide on using two protolysis sites with equal capacities instead of one. This would mean more adjustable parameters, which in turn means improved data fitting. Using two sites and no electrostatic term are the discerning features of the model, which forms a relatively simple basis for the model. The main equations to consider are the protolysis and deprotonation reactions (eq. 10-12) and the intrinsic adsorption constant (eq. 18). Additional parameters that are required are the site capacities.

The CE part of the model was introduced later to accommodate the cation exchange reactions as well<sup>52</sup>. The basic cation exchange reaction for metals A and B on a mineral M is written as:



For this reaction, a thermodynamic constant  $K_T$  can be defined with the Gaines and Thomas convention:

$$K_T = \frac{(N_B)}{(N_A)} * \frac{(f_B)}{(f_A)} * \frac{[A]}{[B]} * \frac{(\gamma_A)}{(\gamma_B)} = K_c * \frac{(f_B)}{(f_A)} \quad (28)$$

where  $N_A$  and  $N_B$  are equivalent fractional occupancies, which are essentially equal to A or B sorbed per kilogram divided by the cation exchange capacity (CEC) and  $f_A$  and  $f_B$  are the surface activity coefficients which are not well defined and may vary.  $[A]$  and  $[B]$  are the aqueous concentrations,  $\gamma_A$  and  $\gamma_B$  are the aqueous phase activity coefficients and  $K_c$  is the selectivity coefficient. The selectivity coefficient can be obtained by calculating from experimental data:

$$K_c = K_d^B * \frac{z_B}{CEC z_a} * [A] * \frac{(\gamma_A)}{(\gamma_B)} \quad (29)$$

where  $z_A$  and  $z_B$  are the charges of the metals, which in this example are +1 and  $K_d$  is the distribution coefficient, defined by equation 1.

No matter which model is chosen, a proper software for calculations and fitting is required. PHREEQC is a modeling software especially designed for aqueous geochemical modeling and its development was mostly focused on simulating actual geochemistry that happens in the real world. It is a program written in C language and has a variety of functions for speciation, batch reaction and transport calculations and inverse modeling<sup>53</sup>. Because of these qualities, it is very widely used for modeling metal sorption on minerals.

## 6. Experimental work

Sorption isotherms and the sorption coefficients ( $K_d$ -values) of selenium were obtained with batch sorption experiments. Further information of possible surface complexation and sorption mechanism of selenium was obtained with titration experiments. The studied kaolinite was characterized with XRD and its CEC and SSA values were measured. Sorption data was modeled with PHREEQC.

### 6.1 Materials

Kaolinite that was used for the experiments was store bought. For the experiments, a grain size in the range of 0,071 mm - 0,3 mm was used. The wanted grain size was obtained by milling in a clay mortar and sieving the kaolinite with iron sieves. 50 g of this kaolinite was also purified for later experiments to prevent any possible interference from unwanted ions. The kaolinite was mixed in water and stirred for 45 minutes. Water was then filtered out and replaced with a 0,1M NaOH solution to get the pH to around 9. The mixture was stirred for 30 mins. After stirring, liquids were again removed by filtration and the kaolinite was rinsed with 1M NaNO<sub>3</sub> solution three times. Rinses were removed and replaced with 0,1 M HNO<sub>3</sub> to get the pH to around 3. Mixture was stirred again for 30 minutes and the acidic solution was filtered out. The purified kaolinite was then rinsed with 0,1M NaNO<sub>3</sub> one last time and then stored in a vacuum for drying.

Kaolinite was characterized with XRD at the Geological Survey of Finland. The samples for XRD were air dried for three weeks before measurement.

The specific surface area (SSA) of Kaolinite was measured at Chalmers University with Kr-BET method<sup>54</sup>. Samples were vacuum dried for a month before the measurement.

Cation exchange capacity (CEC) of kaolinite was determined by using barium to replace the cations on kaolinite. This was accomplished by mixing 1g of kaolinite with 10 ml of 0,1 M BaCl<sub>2</sub> solution. After three hours the solution was separated with centrifuge and measured with MP-AES. This method was similar to the one Ma and Eggleton used in their approach to measuring the CEC experimentally<sup>25</sup>. CEC can be calculated followingly:

$$CEC = \sum \frac{C \cdot V \cdot Z}{m \cdot M} \quad (29)$$

where C is the concentration of the exchangeable cation, V is the volume of the solution, Z is the charge of the cation, m is the mass of the rock and M is the molecular weight of the cation.

A low saline groundwater simulant was prepared for the batch experiments. Preparation was done by dissolving  $\text{MgCl}_2 \cdot 6 \text{H}_2\text{O}$ , KCl,  $\text{CaCl}_2 \cdot 2 \text{H}_2\text{O}$ , (99%, VWR chemicals) NaCl,  $\text{Na}_2\text{SO}_4$  and  $\text{NaHCO}_3$  (99%, Fisher scientific) in water and then stirred for an hour. After stirring the pH was adjusted to around 7,8. The groundwater was used as a background to simulate the actual repository groundwater. Final concentrations of the desired ions are listed in table 2.

*Table 2, the elemental composition of the groundwater simulant used in batch sorption experiments*

Ion	mg/l
$\text{SO}_4$	92
Ca	54
K	10
Mg	18
$\text{HCO}_3$	279
Na	302
Cl	351

## 6.2 Batch experiments

Batches were done by making samples of 0,5g of kaolinite and 10 ml of the groundwater simulant. Two duplicate samples were prepared for each sample. The samples were left to equilibrate for two to three weeks. After the equilibration, selenium was added to the samples. The pH values were also measured at this point. Different amounts of selenium was added to obtain a sorption edge. Selenium concentration would range from  $10^{-3} \text{ M}$  to  $10^{-10} \text{ M}$ . For the higher concentrations  $10^{-3} \text{ M}$  to  $10^{-6} \text{ M}$ , only inactive selenium was used as a tracer.  $\text{Na}_2\text{SeO}_3$  (99%, Sigma-Aldrich) solution was prepared for this purpose, with a molarity of 0,051 M and then diluted 10 times. Dilution would be continued until we had all the different concentrations. From these diluted tracers, 0,2 ml was added to the samples to get the wanted amount of selenium.

For samples with wanted concentrations of  $10^{-7} \text{ M}$  to  $10^{-10} \text{ M}$ , radioactive selenium was also added. This was done for easier measurement of the lower concentrations and because of the

lower detection limit of the MP-AES. Se-75 was used for this purpose. The radioactive Se-75 was purchased from the Czech Metrology Institute with gamma impurities < 0,1%. A total activity concentration of around 600 Bq/10 ml of Se-75 was added to the samples; around 40 µl per sample. After adding the selenium, the samples were again left to equilibrate for two weeks. After equilibration, the samples were centrifuged and the solutions were collected and filtered with 0,45 µm syringe filters. The samples that had Se-75 added to them were measured with Hidex AMG gamma counter and the samples with only inactive selenium were measured with ICP-MS (Agilent technologies 7500ce).

### 6.3 Titration experiments

Purified kaolinite was used for the titration experiments, which gives information on the surface complexation of selenium. Titration experiments were done in a low oxygen gas inert glove box filled with nitrogen gas to avoid any possible reactions in regular air conditions. Samples for the titration experiments were a mixture of impurified kaolinite and 0,01 M KClO<sub>4</sub>. A total amount of 20 samples were prepared and left to equilibrate for a few days. After equilibration half of the samples were treated with 0,1 M HNO<sub>3</sub> to adjust the pH lower and the other half with 0,1 M NaOH to adjust the pH higher. The aim was to get an idea of cation and anion exchange on the mineral surfaces, which requires a wide array of samples with different pH values.

After adding the acid/base, the samples were again left to equilibrate for a day. On the next day the pH was measured to see if any changes had happened. Samples were then centrifuged and the supernatant was separated for two different measurements. 15 ml of solution was reserved for the backtitration and another 5 ml was reserved for cation measurement. Backtitration was done to finalize the cation and anion exchange after which the samples and were measured with MP-AES (Agilent Technologies 4200). The other 5 ml solution that was reserved was also measured with MP-AES.

## 7. Results and discussion

### 7.1 Results of mineral characterizations

The kaolinite was characterized with XRD. The mineral composition was found to be almost entirely kaolinite, with only trace amounts of other clay minerals such as illite. A diffractogram can be seen in figure 8. The fact that kaolinite proved to be relatively pure is promising for the future modeling approach.

#### Kaolinite

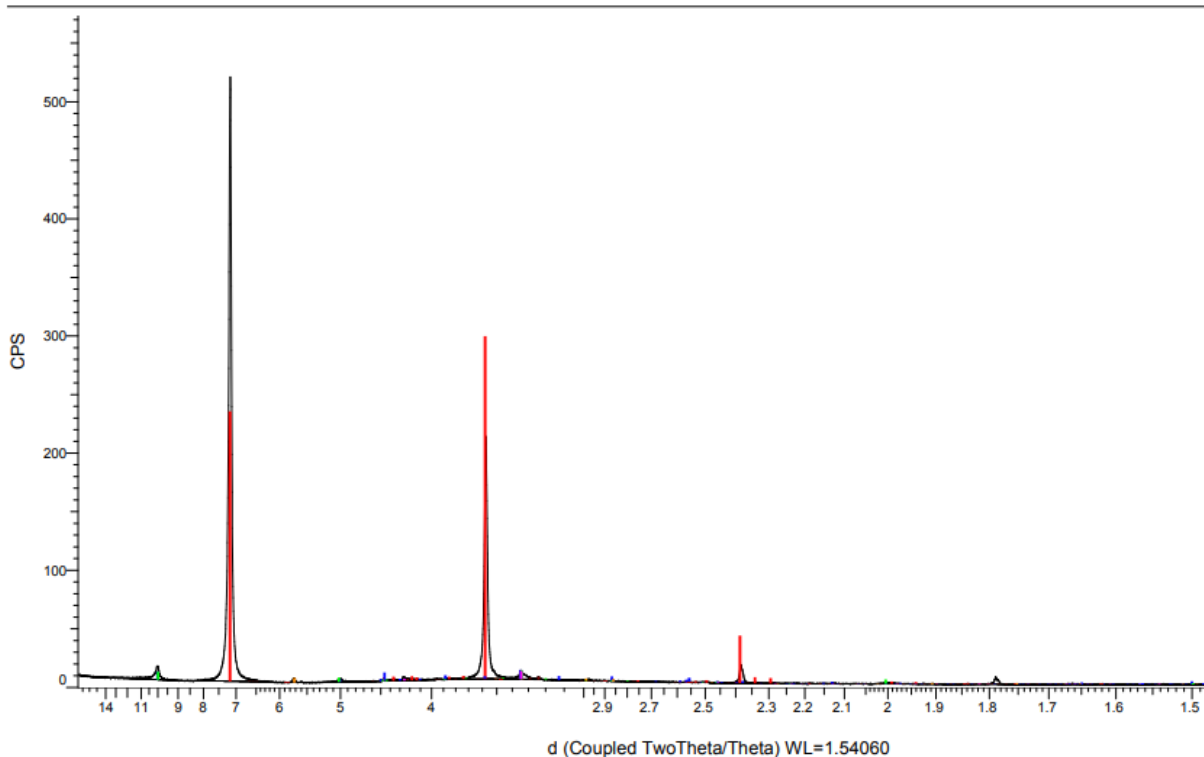


Fig 8, a diffractogram of kaolinite from the XRD. Red spikes are from kaolinite, which is the dominant mineral. A small green peak at 10 Å indicates some other mineral such as illite or a mica.

The CEC was calculated from the MP-AES results. The measurement yielded concentrations for the different cations, which were then added up for the final CEC value. The CEC and SSA values are recorded to be 26,1 meq/kg for CEC and 7,61 m<sup>2</sup>/g for SSA.

## 7.2 Results of batch sorption experiments

$K_d$ -values were obtained for different concentrations of selenium from the batch sorption experiments. ICP-MS yielded concentration results for the higher initial concentrations and the gamma counter for the lower initial concentrations. These results were used to calculate the final  $K_d$ -values. The resulting sorption isotherm can be seen in figure 9. The isotherm follows the expected trend of higher sorption at lower concentrations, with a drop in sorption as the concentration increases. Main source for errors is the accuracy of the measuring equipment (ICP-MS, gamma counter).

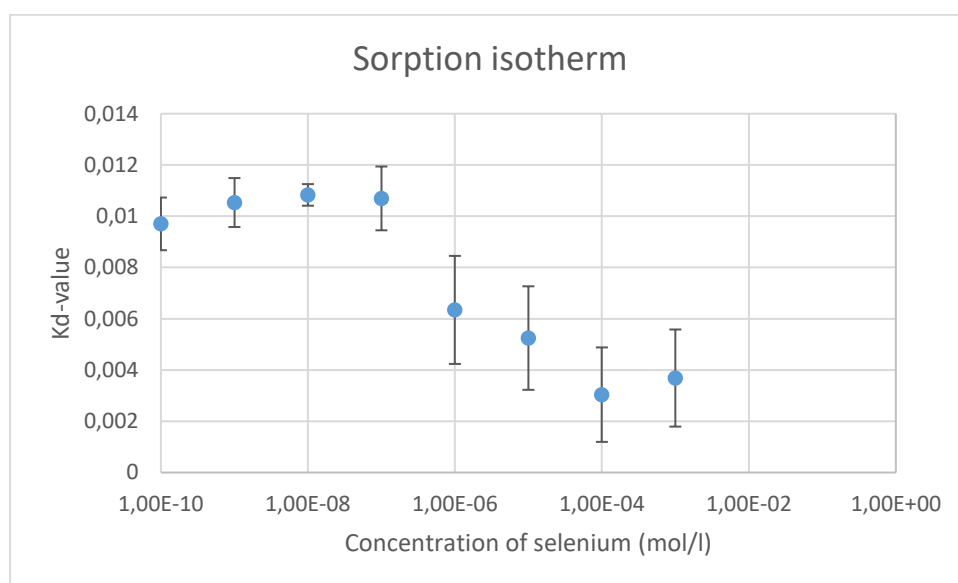


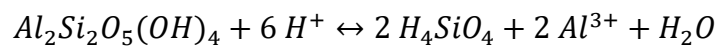
Fig 9. The sorption isotherm of selenium(IV) on kaolinite with errors

The sorption data implies, that Se(IV) doesn't sorb very well on the kaolinite surface. Kaolinite itself does not reduce the mobility of selenium so its sorption left limited to just surface complexation, which can only happen on the available sorption surfaces. Also, the  $K_d$  was expected to be higher than the results at all points because of kaolinites similar sorption behavior to biotite. Li et al. recorded higher  $K_d$ -values for selenium sorption on biotite using the same methods<sup>41</sup>. Ervanne et al. obtained  $K_d$ -values<sup>11</sup> ranging from  $11 \cdot 10^{-3}$  to  $720 \cdot 10^{-3} \text{ m}^3/\text{kg}$ , compared to the lower values of  $3 \cdot 11 \cdot 10^{-3} \text{ m}^3/\text{kg}$  obtained here with differences coming from the background solutions that were used.

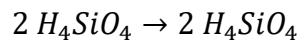
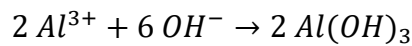
### 7.3 Results of titration experiments

To better understand the sorption behaviors of Se on kaolinite and provide basic parameters for future modelling practices, titration experiments were performed following the batch sorption experiments. The titration experiments were carried out by a batch-wise manner together with a backtitration process. The information of kaolinite dissolution and protonation reactions on kaolinite surfaces can be provided by the titration results.

The dissolution of kaolinite during the titration process can be described by a dissolution reaction:

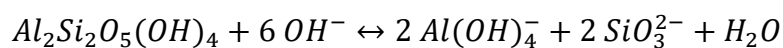


During backtitration, it can then be described by the consumption of  $OH^-$  group. In this case, only the aluminum is affected:

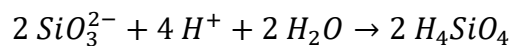
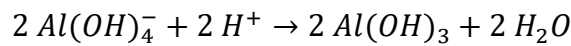


We can see that for 6  $H^+$  consumed during the dissolution of kaolinite, another 6  $OH^-$  are consumed during the backtitration, making the equations equal.

The dissolution of kaolinite in alkaline conditions can be described by another dissolution reaction:



And backtitration again by consumption of the  $H^+$ , with now both silicate and aluminum reacting:



This time 6  $OH^-$  groups are consumed during the dissolution and 6  $H^+$  are consumed during the backtitration according to the equations above. Again, the reaction equations are equal. This means that all the hydroxide ions and protons are produced and consumed during the titration process, indicating that proton exchange and cation exchange are the main processes that affect the titration.



Five cations were analyzed from the titration samples: silicon, sodium, aluminum, magnesium and calcium. The analysis results are shown in figure 10. Sodium was excluded from the figure because of its much higher concentration compared to the other cations. The excess sodium is from the purification process of the kaolinite, where sodium hydroxide and sodium nitrate were both used. Silicon was instead excluded because no amount of silicon was detected from the samples. This is curious because silicon should be prevalent after the kaolinite dissolves along with aluminum. The other cations behave as expected. Magnesium and calcium concentrations decrease as pH increases, while aluminum concentration is seemingly high at both high and low pH. This indicates dissolution of kaolinite at these conditions.

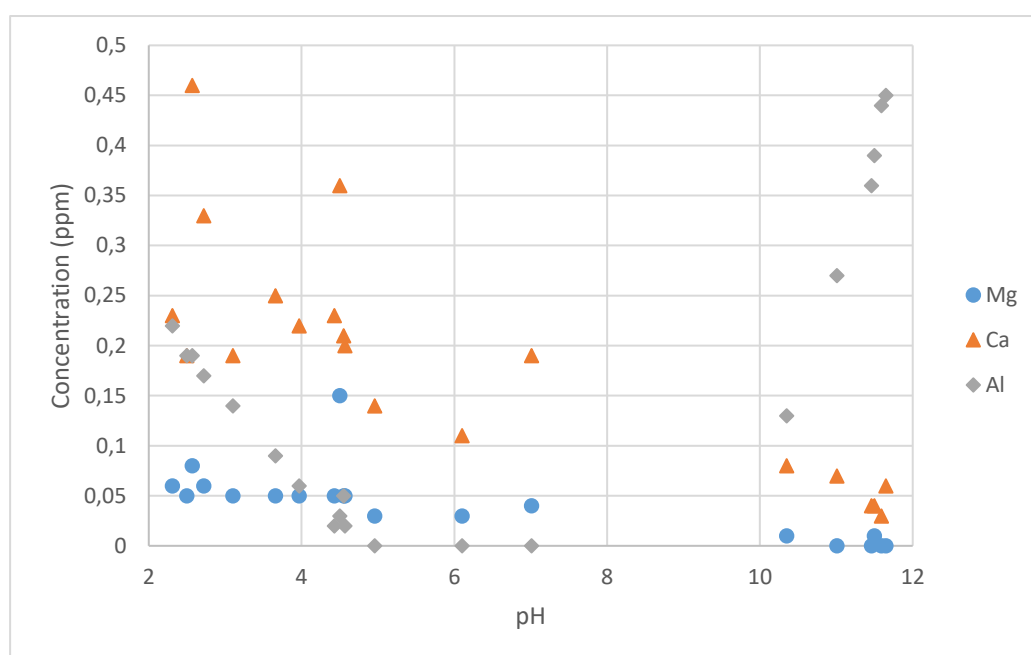
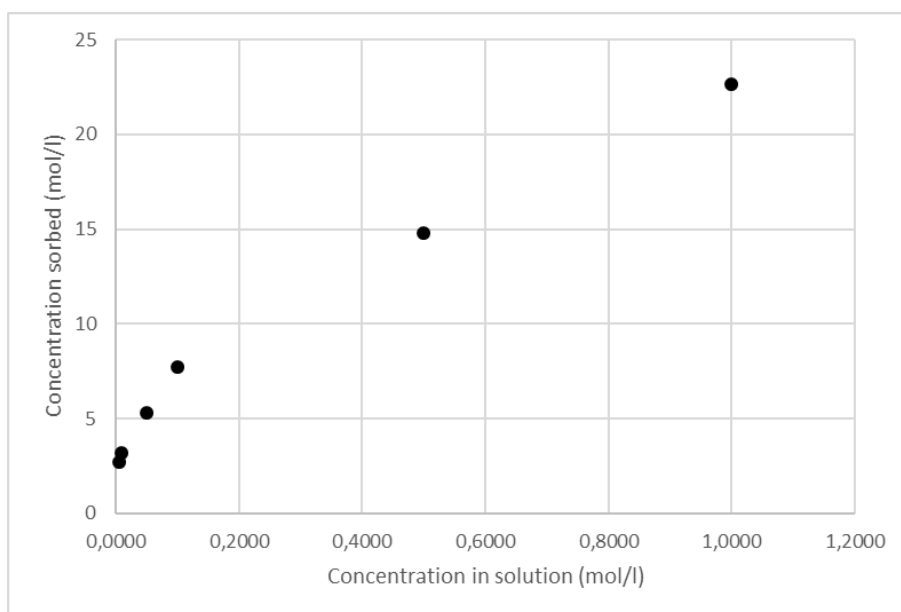


Fig 10, cation concentration as a function of pH in titration experiments.

The titration results calibrated by the backtitration and mineral dissolution data are shown in figure 12. It is clear that the amount of  $H^+$  and  $OH^-$  consumed at  $pH < 3$  and  $pH > 11$  increased quickly. Thus, the titration results require more factors for the calibration of the curve. Cation exchange and proton exchange reactions affect the titration in addition to backtitration and dissolution. By recording the cation exchange abilities of different cations with  $Na^+$  on kaolinite surface, the corresponding selectivity coefficients of the cation exchange reactions could be measured (Table 4). The selectivity coefficient of the proton exchange reaction is assumed to be one, since the study of the exchange reactions of hydrogen ions is greatly complicated

because of the instability of the mineral. Combined with the measured CEC value and the equilibrium concentration of different cations in the supernatant, the amount of sorption sites occupied by different cations on kaolinite surface can be calculated (Table 5).). The results show that  $\text{Al}^{3+}$  is the most abundant cation that is sorbed on kaolinite surface. Thus, aluminum and proton occupancies are used for the aforementioned cation and proton exchange effect corrections. Aluminum sorption data from the backtitration experiment can be seen in figure 11.



*Fig 11, aluminum sorption data from backtitration experiment.*

After calibrations of all the factors mentioned above (backtitration, mineral dissolution, cation exchange and proton exchange), the net consumed amounts of  $\text{H}^+$  and  $\text{OH}^-$  as a function of pH are shown in figure 12. The calibrated titration curve can then be modeled according to protonation reactions. Equations 10 and 11 together with the CEC and SSA can be derived for each of the different types of sorption sites along with the protonation and deprotonation constants.

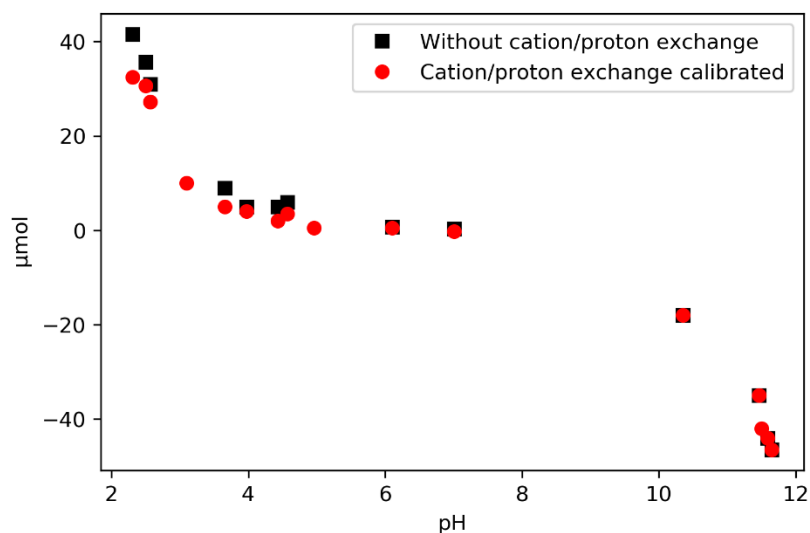


Fig 12, Data for Se(IV) from titration experiment calibrated by backtitration and mineral dissolution data (▪) and modelled including all the factors (●) on converted kaolinite in 0.01 M KClO<sub>4</sub> solution from pH 3 to pH 12.

Table 3, Cation exchange reactions of the dissolved cations with Na<sup>+</sup> on kaolinite surface and the calculated selectivity coefficients according to the Gaines and Thomas convection.

Cation exchange reaction	Selectivity coefficients (K)
Na-kaolinite + H <sup>+</sup> = H-kaolinite+ Na <sup>+</sup>	1 (logK=0)
Na-kaolinite+ K <sup>+</sup> =K-kaolinite+ Na <sup>+</sup>	-5.077
2Na-kaolinite+ Mg <sup>2+</sup> = Mg-kaolinite+ 2Na <sup>+</sup>	0.310
2Na-kaolinite+ Ca <sup>2+</sup> = Ca-kaolinite+ 2Na <sup>+</sup>	0.569
3Na-kaolinite + Al <sup>3+</sup> = Al-kaolinite + 3K <sup>+</sup>	0.994

Table 4, The amount of sorption sites occupied by cations on converted kaolinite.

pH	Cation occupancies (mol/Kg)				
	H	Ca	Mg	Na	Al
3.97	0.00017	0.00084	0.00017	0.0016	0.0137
3.66	0.00029	0.00073	0.00013	0.0014	0.0138
2.72	0.0020	0.00062	0.00010	0.0011	0.0134
2.57	0.0028	0.00079	0.00012	0.0010	0.0131
2.50	0.0033	0.00033	0.00008	0.0010	0.0132
2.31	0.0048	0.00035	0.00008	0.0010	0.0128

## 8. Conclusions

In short, the results are summed up here.

Kaolinite's characteristics were studied by measuring three specific parameters: the mineral composition, CEC and SSA. XRD data shows that the kaolinite was very pure while the experimentally determined CEC and SSA were used successfully in the calibration of the titration curve.

A sorption isotherm of selenium on kaolinite was obtained from batch sorption experiments. The isotherm follows the expected trend, indicating a generally low sorption of selenium on kaolinite. Lower  $K_d$  -values compared to previous studies can be explained by the differences in background solution.

The results from titration experiments show a rapid increase of  $H^+$  and  $OH^-$  consumption at low and high pH values respectively. A fully calibrated curve showing the extent of the aforementioned ion consumption was finally obtained by including backtitration and mineral dissolution data.

Overall, the experiments were successful and useful data was obtained for sorption modeling in the future.

## 9. Future work

The parameters determined in this work will be used for the modeling of selenium sorption on kaolinite in the future and the model will be developed further using the results obtained here.

The sorption edge is important for fully understanding the sorption behavior and it is required for a more complete sorption model. While the sorption isotherm itself already gives good insight on the sorption properties of Se(IV) on kaolinite, the sorption edge would further help support the findings. It would also be rather simple to do the sorption edge determination as a follow-up to this study.

The mobility of Se(IV) should be considered for studying. Diffusion of selenium in near-surface geological environments has not been studied a whole lot yet but should be worth considering

due to its current relevance. This would require more planning and setup for the experiments than the sorption edge determination.

Structural information for the sorbed species could also be further studied, along with the retardation mechanisms of Se(IV). This was also considered for this study but again was left out due to time constraints, but also because of unavailable measuring equipment. X-ray absorption spectroscopy and Extended X-ray adsorption fine structure would be excellent tools for studying the species structures and should be considered for further research.

## References

- 1 A. Poteri, H. Nordman and V. Pulkkanen, *Radionuclide Transport in the Repository Near-Field and Far-Field*, Posiva Oy, 2014.
- 2 P. Sellin and O. X. Leupin, *Clays and Clay Minerals*, 2013, **61**, 477-498.
- 3 SKB, Environmental Impact Statement, Interim storage, encapsulation and final disposal of spent nuclear fuel, 2011
- 4 R. Haapanen, L. Aro, J. Helin, T. Hjerpe, A. Ikonen, T. Kirkkala, S. Koivunen, A.-M. Lahdenperä, L. Puhakka, M. Rinne and T. Salo, *Olkiluoto Biosphere Description 2009*, 2009.
- 5 R. Brennetot, L. Pierry, T. Atamyan, G. Favre and D. Vailhen, *Journal of Analytical Atomic Spectrometry*, 2008, **23**, 135-1358.
- 6 J. Lehto and X. Hou, *Chemistry and analysis of radionuclides*, Wiley-VCH, Weinheim, 2011.
- 7 M. Martínez, J. Giménez, J. de Pablo, M. Rovira and L. Duro, *Applied Surface Science*, 2006, **252**, 3767-3773.
- 8 J. Ikonen, M. Voutilainen, M. Söderlund, L. Jokelainen, M. Siitari-Kauppi and A. Martin, *Journal of Contaminant Hydrology*, 2016, **192**, 203-211 (DOI:10.1016/j.jconhyd.2016.08.003).
- 9 M. Rovira, J. Giménez, M. Martínez, X. Martínez-Lladó, J. de Pablo, V. Martí and L. Duro, *Sorption of selenium(IV) and selenium(VI) onto natural iron oxides: Goethite and hematite*, 2007.
- 10 I. Aaltonen, J. Engström, K. Front, S. Gehör, P. Kosunen, A. Kärki, M. Paananen, S. Paulamäki and M. Mattila, *Geology of Olkiluoto*, Posiva Oy, 2016.
- 11 H. Ervanne, M. Hakanen and J. Lehto, *J Radioanal Nucl Chem*, 2016, **307**, 1365-1373.

- 12 X. Li, E. Puhakka, J. Ikonen, M. Söderlund, A. Lindberg, S. Holgersson, A. Martin and M. Siitari-Kauppi, *Applied Geochemistry*, 2018, **95**, 147-157.
- 13 E. Muuri, M. Matara-aho, E. Puhakka, J. Ikonen, A. Martin, L. Koskinen and M. Siitari-Kauppi, *Applied Geochemistry*, 2018, **89**, 138-149.
- 14 R. C. Ewing, *Nature materials*, 2015, **14**, 252-257.
- 15 M. Herod, *GeoPoll: What should we do with radioactive waste?*, 2015.
- 16 B. Grambow, *Journal of Contaminant Hydrology*, 2008, **102**, 180-186.
- 17 H. J. Ervanne, M. E. Hakanen and E. J. Puukko, *Safety Case for the Disposal of Spent Nuclear Fuel at Olkiluoto*, Posiva, 2014.
- 18 G. Sinnathamby, L. Korkiala-Tanttu and J. Gallardo Forés, *Soils and Foundations*, 2014, **54**, 777-788.
- 19 H. J. Ervanne, M. E. Hakanen and E. J. Puukko, *Safety Case for the Disposal of Spent Nuclear Fuel at Olkiluoto*, Posiva, 2014.
- 20 National Institutes of Health, Office of Dietary Supplements, <https://ods.od.nih.gov/factsheets/selenium-HealthProfessional/#h7>, (accessed 12.8. 2019).
- 21 C. G. Wilber, *Clinical Toxicology*, 1980, **17**, 171-230.
- 22 N. Jordan, C. Lomenech, N. Marmier, E. Giffaut and J. -. Ehrhardt, *Sorption of Selenium(IV) in the presence of aqueous silicates species on iron corrosion product in underground radwaste repository conditions*, La Baule, France, 2007.
- 23 P. De Canniere, A. Maes, S. Williams, C. Bruggeman, T. Beauwens, N. Maes and M. Cowper, *Behaviour of Selenium in Boom Clay*, Belgium, 2010.
- 24 J. W. Anthony, *Handbook of Mineralogy: Silica, silicates*, Mineral Data Publishing, Chantilly, Virginia, 1995.
- 25 C. Ma and R. Eggleton, *Clays Clay Miner*, 1999, **47**, 174-180.
- 26 Kaolinite mineral data, [webmineral.com/data/Kaolinite.shtml](http://webmineral.com/data/Kaolinite.shtml), (accessed Nov 20, 2019).
- 27 H. Mei, Y. Meng, Y. Gong, X. Chen, C. Chen and X. Tan, *J Radioanal Nucl Chem*, 2017, **311**, 1899-1907.
- 28 Z. Hou, K. Shi, X. Wang, Y. Ye, Z. Guo and W. Wu, *J Radioanal Nucl Chem*, 2015, **303**, 25-31.
- 29 W. Xiangke, D. Wenming, G. Yingchun, W. Changhui and T. Zuyi, *Journal of Radioanalytical and Nuclear Chemistry*, 2001, **250**, 267-270.

- 30 D. K. Bhumbra, S. S. Dhaliwal, K. S. Sajwan and B. S. Sekhon, in *Chemistry of Trace Elements in Fly Ash*, ed. nonymous , Springer, Boston, MA, 2003, p. 237-249.
- 31 M. E. Essington, *Soil and water chemistry*, CRC Press, Boca Raton [u.a.], 2004.
- 32 T. E. Payne, V. Brendler, M. Ochs, B. Baeyens, P. L. Brown, J. A. Davis, C. Ekberg, D. A. Kulik, J. Lutzenkirchen, T. Missana, Y. Tachi, L. R. Van Loon and S. Altmann, *Environmental Modelling and Software*, 2013, **42**, 143-156.
- 33 S. Goldberg, L. J. Criscenti, D. R. Turner, J. A. Davis and K. J. Cantrell, *Vadose Zone Journal*, 2007, **6**, 407.
- 34 F. Morel, *Principles of aquatic chemistry*, J. Wiley, New York, 1983.
- 35 D. Peak and D. L. Sparks, *Environmental science & technology*, 2002, **36**, 1460-1466.
- 36 D. Peak, *Journal of Colloid And Interface Science*, 2006, **303**, 337-345.
- 37 T. Missana, U. Alonso, A. C. Scheinost, N. Granizo and M. García-Gutiérrez, *Geochimica et Cosmochimica Acta*, 2009, **73**, 6205-6217.
- 38 M. Duc, G. Lefevre, M. Fedoroff, J. Jeanjean, J. C. Rouchaud, F. Monteil-Rivera, J. Dumonceau and S. Milonjic, *Journal of Environmental Radioactivity*, 2003, **70**, 61-72.
- 39 M. Söderlund, *Sorption and speciation of radionuclides in boreal forest soil*, University of Helsinki, 2016.
- 40 X. Yang, X. Ge, J. He, C. Wang, L. Qi, X. Wang and C. Liu, *Environmental Science & Technology*, 2018, **52**, 1320-1329.
- 41 X. Li, E. Puhakka, L. Liu, W. Zhang, J. Ikonen, A. Lindberg and M. Siitari-Kauppi, *Chemical Geology*, 2020, **533**, 119433.
- 42 C. A. J. Appelo and D. Postma, *Geochemistry, groundwater and pollution*, Balkema, Leiden [u.a.], 2006.
- 43 OECD, *Thermodynamic Sorption Modelling in Support of Radioactive Waste Disposal Safety Cases: NEA Sorption Project Phase III*, Nuclear Energy Agency, Paris, 2012.
- 44 M. H. Bradbury and B. Baeyens, in *Interface Science and Technology*, ed. nonymous , Elsevier Science & Technology, 2006, p. 518-538.
- 45 B. Arora, J. A. Davis, N. F. Spycher, W. Dong and H. M. Wainwright, *Groundwater*, 2018, **56**, 73-86.
- 46 J. Lützenkirchen, *Journal of Colloid And Interface Science*, 1999, **217**, 8-18.

47 S. Goldberg and D. L. Suarez, in *Interface Science and Technology*, ed. anonymous , Elsevier Science & Technology, 2006, p. 491-517.

48 M. B. Gabos, S. Goldberg and L. R. F. Alleoni, *Environmental Toxicology and Chemistry*, 2014, **33**, 2197-2207.

49 M. Villalobos, in *Interface Science and Technology*, ed. anonymous , Elsevier Science & Technology, 2006, p. 417-442.

50 S. Goldberg, *Soil Science Society of America Journal*, 2013, **77**, 64.

51 M. Bradbury and B. Baeyens, *A Quantitative Mechanistic Description of Ni, Zn and Ca Sorption on Na-Montmorillonite Part III: Modeling*, Wurelingen, 1995.

52 M. H. Bradbury and B. Baeyens, *Geochimica et Cosmochimica Acta*, 2005, **69**, 875-892.

53 D. Parkhurst and T. Appelo, *User's guide to PHREEQC version 3 - a computer program for speciation, batch-reaction, one-dimensional transport, and inverse geochemical calculations*, 1999.

54 I. Dubois, S. Holgersson, S. Allard and M. Malmström, *Proc. Radiochimica Acta*, 2011, **1**, 75-82.



## Appendices

*Appendix 1, Data from the gamma counting of batch experiment samples*

Sample	Counted time (s)	Se-75 (counts)	Se-75 (CPM)	Se-75 (Bq)
blank	600	30395	3040	51
blank	600	30499	3050	51
10 <sup>-7</sup>	600	24794	2480	41
10 <sup>-7</sup>	600	26683	2669	44
10 <sup>-7</sup>	600	25182	2518	42
blank	600	30396	3040	51
blank	600	29809	2981	50
10 <sup>-8</sup>	600	25474	2548	42
10 <sup>-8</sup>	600	25274	2528	42
10 <sup>-8</sup>	600	24826	2483	41
blank	600	29475	2948	49
blank	600	29114	2912	49
10 <sup>-9</sup>	600	24638	2464	41
10 <sup>-9</sup>	600	26104	2611	44
10 <sup>-9</sup>	600	25215	2522	42
blank	600	27751	2775	46
blank	600	28492	2849	47
10 <sup>-10</sup>	600	23960	2396	40
10 <sup>-10</sup>	600	25426	2543	42
10 <sup>-10</sup>	600	25159	2516	42
background	600	2520	252	4

*Appendix 2, Data from ICP-MS measurement of batch experiment samples*

Sample Name	Vial Number	Type	Conc. [ ppb ]
std 1	1102	CalStd	0,92456
std 5	1103	CalStd	4,78879
std 10	1104	CalStd	10,69349
std 20	1105	CalStd	19,70983
3.1	1106	Sample	5,44754
3.2	1107	Sample	6,51889
3.3	1108	Sample	6,82272
4.1	1109	Sample	6,39229
4.2	1110	Sample	7,37552
4.3	1111	Sample	6,86609
5.1	1112	Sample	6,5172
5.2	1201	Sample	6,06421
5.3	1202	Sample	6,20116
6.1	1203	Sample	5,69022
6.2	1204	Sample	6,05739
6.3	1205	Sample	6,26373